ELSEVIER

International Journal of Solids and Structures 41 (2004) 365–384

INTERNATIONAL JOURNAL OF SOLIDS and STRUCTURES

www.elsevier.com/locate/ijsolstr

Nonlinear dynamic analysis of composite laminated plates containing spatially oriented short fibers

K.K. Shukla [a], Jhao-Ming Chen [b], Jin H. Huang [b,*]

[a] *Applied Mechanics Department, M.N.N.I.T, Allahabad-04, India*

[b] *Department of Mechanical and Computer-Aided Engineering, Feng Chia University, 100 Wen-Hwa Road, Taichung 407, Taiwan*

Received 14 April 2003; received in revised form 19 September 2003

Abstract

The paper presents an analytical approach to examine the nonlinear dynamic responses of a laminated composite plate composed of spatially oriented short fibers in each layer of the composite. Using Mori–Tanaka mean field theory, the effective elastic moduli of each lamina are obtained explicitly as a function of the properties of the constituents, volume fraction, orientation angles, and fiber shape. The resulting moduli are further applied to analyze the nonlinear transient response of the laminated plate. The formulation is based on Mindlin first-order shear deformation theory and von-Karman nonlinear kinematics, and the methodology of the solution utilizes the fast converging finite double Chebyshev series. Houbolt time marching scheme and quadratic extrapolation technique are used for the temporal discretization and linearization, respectively. Numerical results are presented for laminated plates made of E-glass/Epoxy fiber reinforced composites.

Keywords: Nonlinear dynamic response; Laminated composite plate; Spatial short fibers; Chebyshev series

1. Introduction

Fiber composite laminates have found many applications in variety of engineering structures ranging from deep ocean to high in the sky and fiber architecture has been considered to be the most important feature in the composite design. Optimum placement of the fibers depending upon the requirements is a direct and efficient way to improve the composite performance under various conditions. Depending upon the structural requirements, environmental and loading conditions, the orientations of the fibers in the composites may be linear, planar, or spatial. Out of these, the composites containing spatially distributed fibers are finding wide variety of applications due to their more balanced properties, which lead to an improved through-the-thickness stiffness/strength. However, it is very difficult to control the movement of

* Corresponding author. Tel.: +886-2451-7250; fax: +886-2451-6545.
E-mail address: jhhuang@fcu.edu.tw (J.H. Huang).

0020-7683/$ - see front matter © 2003 Elsevier Ltd. All rights reserved.
doi:10.1016/j.ijsolstr.2003.09.042

fibers in a perfect alignment and therefore there is a need of a probabilistic study on the orientation of fibers in the composite. The fiber distribution in the composites can be represented by either a density function or a cumulative function, which helps in computing the elastic constants of the composite effectively.

Several approaches have been proposed for evaluating the effective elastic properties. Eshelby (1957) proposed a method for evaluating effective elastic constants and it is quite reasonable when the fiber volume fraction is small. Halpin et al. (1971) and Christensen and Malls (1972) proposed aggregate models for irregular fiber orientation and these models predict elastic properties effectively when the volume fraction of the fiber is significant. But, these models do not reflect the geometrical aspects of the inclusion. The method proposed by Mori and Tanaka (1973) is supposed to be one of the most powerful methods for predicting the overall behavior of the composite material containing nondilute concentration of inclusions. Taya and Chou (1981) proposed a method for computing overall stiffness of a three-phase composite which are of isotropic materials. Beveniste (1987) successfully applied the Mori–Tanaka method to investigate the stress and strain concentration tensors and effective elastic moduli of a composite. Weng (1990) concluded that the Mori–Tanaka method can be safely applied to obtain the elastic moduli of identical shaped multiphase composite with inclusions. Based on Mori–Tanaka mean field theory, analytical expressions are presented in the present paper for evaluation of effective moduli of composites reinforced with different orientations of short fibers. A probability density function controlled by three Euler's angles is introduced to simulate spatial fiber orientation in a preferred direction.

The nonlinear dynamic behavior of the laminated composite plates/panels in response to the conditions they are subjected to, have received considerable attention in the past. Some excellent reviews and monographs on the vibrations of plates are presented by Sathyamoorthy (1987), Yamada and Irie (1987), and Leissa (1998). A number of investigations have been carried out on the nonlinear dynamic analysis of the laminated composite plates and notably among them are due to Reddy (1983), Bhimaraddi (1992), Shi et al. (1997), Cheng et al. (1993), Khdeir and Reddy (1999), Singh and Rao (2000), Nath and Shukla (2001), and many others. Huang (2001) presented a micromechanics based approach for the linear dynamic analysis of laminated composite plate composed of randomly oriented fibers. From the available literatures, it is evident that most of the studies are related to the nonlinear vibration analysis of the composite laminated plates containing long fibers employing numerical techniques.

In the preset paper, nonlinear dynamic responses of composite laminated plates containing spatially oriented short fibers are carried out analytically, employing fast converging finite double Chebyshev series. A Chebyshev series always has the property of infinite order convergence even for the functions that are nonperiodic and it eliminates the terminal discontinuities. It uses the global basis functions in which each basis function is a polynomial of high degree, which is not zero, except for isolated points over the entire computational domain (Rivilin, 1974). When fast iterative matrix solvers are used, this method can be much more efficient than numerical techniques for several classes of problems. The effects of fiber orientations, fiber aspect ratio, fiber volume fraction, and lamination scheme on the nonlinear dynamic responses of the composite laminated plate are studied. The numerical results for E-glass/Epoxy fiber reinforced composite laminated plates with all edges clamped (CCCC) and two opposite edges clamped and two simply supported (CCSS) are presented.

2. Mathematical formulation

The laminated composite rectangular plate made up of n layers with composites containing spatial short fibers is shown in Fig. 1. Perfect bonding between the layers is assumed. Effective elastic properties of the composites are evaluated employing the Mori–Tanaka mean field theory and the governing equations of motion of the composite laminated plates are presented in the following subsections.

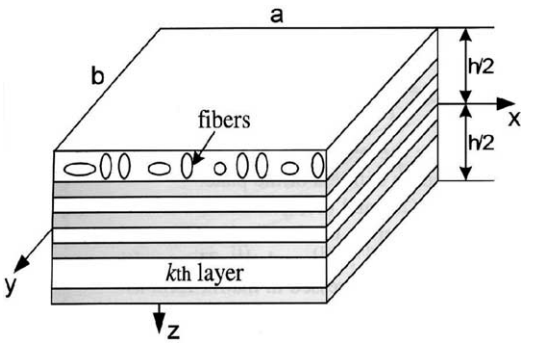

Fig. 1. Composite laminated plate containing random short fibers.

2.1. Effective elastic properties

For obtaining the effective properties of a reinforced composite, a sufficiently large two-phase composite D consisting of randomly oriented spatial inhomogeneities $\Omega\ (=\Omega_1+\Omega_2+\cdots+\Omega_N)$ with elastic constants C^2_{ijmn} and volume fraction f is considered. The surrounding matrix is denoted by D–Ω and has elastic constants C^1_{ijmn}. To deal with such a composite with randomly oriented spatial inclusions, the Mori–Tanaka mean field theory is employed to predict the effective elastic moduli of the composite. An advantage of using this theory is that the resulting moduli satisfy self-consistency, i.e., this theory generally yields the same effective elastic moduli for the cases when either a traction or displacement field is prescribed on the boundary of the composite (Huang and Kuo, 1996). Consequently, the estimation of effective elastic moduli can be carried out independently of the far field boundary conditions. This is strongly desirable from physical viewpoint.

Considering the case where the displacement at the boundary of a composite body D is prescribed, so that the uniform strain ε^0_{mn} is given. In the absence of the inhomogeneities, the prescribed strain produces the uniform stress, σ^0_{ij}. When a large number of inhomogeneities are introduced into D, the strain changes to $\varepsilon^0_{mn}+\varepsilon_{mn}$, and the stress to $\sigma^0_{ij}+\sigma_{ij}$. Here ε_{mn} denotes the disturbed strain, and σ_{ij} stands for the disturbed stress. The averages of these quantities are expressed by $\langle\varepsilon_{mn}\rangle_M$ and $\langle\varepsilon_{mn}\rangle_\Omega$ for the matrix and the inhomogeneities, respectively. Since the surface strain is prescribed, the volume average of the disturbed strain must vanish, which yields

$$(1-f)\langle\varepsilon_{mn}\rangle_M + f\langle\varepsilon_{mn}\rangle_\Omega = 0 \tag{1}$$

The presence of a large number of the inhomogeneities ensures that the addition of a new inhomogeneity does not change $\langle\varepsilon_{mn}\rangle_M$ and $\langle\varepsilon_{mn}\rangle_\Omega$. Thus, an inhomogeneity Ω_k is inserted into a region where the insertion is allowed. The strain in Ω_k consists of two parts. The first part is the strain $\langle\varepsilon_{mn}\rangle_M$, which have existed before the insertion. The second part is the strain ε_{mn} in the inserted inhomogeneity, calculated only when this inhomogeneity is present. Thus, the sum of the first and second parts, in Ω_k becomes

$$\langle\varepsilon_{mn}\rangle_{\Omega_k} = \langle\varepsilon_{mn}\rangle_M + \varepsilon_{mn} \tag{2}$$

Then, the average of the disturbed stress in the matrix and the kth inhomogeneity are respectively written as

$$\langle\sigma_{ij}\rangle_M = C^1_{ijmn}\varepsilon_{mn} \tag{3}$$

$$\langle\sigma_{ij}\rangle_{\Omega_k} = C^2_{ijmn}(\langle\varepsilon_{mn}\rangle_M + \varepsilon_{mn}) \tag{4}$$

where superscripts 1 and 2 denote for the matrix and inclusions, respectively.

Since the composite is subjected to the uniform far-field strain ε^0_{mn}, the average stress in the kth inhomogeneity can be expressed as

$$\sigma^0_{ij} + \langle \sigma_{ij} \rangle_{\Omega_k} = C^2_{ijmn}(\varepsilon^0_{mn} + \langle \varepsilon_{mn} \rangle_M + \varepsilon_{mn}) \tag{5}$$

By means of the equivalent method (Eshelby, 1957), the stress in the inhomogeneity can be simulated by those in an equivalent inclusion with the elastic constants of the matrix and a fictitious eigenstrain ε^*_{mn} (Mura, 1987). Hence, Eq. (5) can be rewritten as

$$\begin{aligned} \sigma^0_{ij} + \langle \sigma_{ij} \rangle_{\Omega_k} &= C^2_{ijmn}(\varepsilon^0_{mn} + \langle \varepsilon_{mn} \rangle_M + \varepsilon_{mn}) \\ &= C^1_{ijmn}(\varepsilon^0_{mn} + \langle \varepsilon_{mn} \rangle_M + \varepsilon_{mn} - \varepsilon^*_{mn}) \end{aligned} \tag{6}$$

Since the applied load is uniform and the inhomogeneity is spatial, the disturbed strain ε_{mn} in the preceding equation can be related to the fictitious eigenstrain ε^*_{mn} by

$$\varepsilon_{mn} = S_{mnab}\varepsilon^*_{ab} \tag{7}$$

with S_{mnab} being the Eshelby tensors (Mura, 1987). With the aid of Eqs. (6) and (7), it is written as

$$\langle \varepsilon_{mn} \rangle_{\Omega_k} = \langle \varepsilon_{mn} \rangle_M + S_{mnab}\varepsilon^*_{ab} \tag{8}$$

Substituting Eq. (8) into (1), the average strain in the matrix is written as

$$\langle \varepsilon_{mn} \rangle_M = -fS_{mnab}\varepsilon^*_{ab} \tag{9}$$

The equivalent eigenstrain ε^*_{mn} solved by substitution of Eqs. (8) and (9) into the equivalent condition (6) is

$$\varepsilon^*_{ab} = -V^{-1}_{abij}(C^2_{ijmn} - C^1_{ijmn})\varepsilon^0_{Mn} \tag{10}$$

where V^{-1}_{abij} is the inverse of V_{ijab} defined by

$$V_{ijab} = (1-f)(C^2_{ijmn} - C^1_{ijmn})S_{mnab} + C^1_{ijab} \tag{11}$$

Since all inhomogeneities are of the same shape with the same material properties, the average of equivalent eigenstrain ε^*_{mn} in Ω_k is the same as that over Ω. Consequently, the average value over Ω_k is identical with that over Ω, namely, $\langle \varepsilon_{mn} \rangle_{\Omega_k} = \langle \varepsilon_{mn} \rangle_{\Omega}$. Then, the overall stress $\langle \sigma_{ij} \rangle_C$ of the composite by averaging those of the inhomogeneities and the matrix is defined as

$$\langle \sigma_{ij} \rangle_C = \sigma^0_{ij} + (1-f)\langle \sigma_{ij} \rangle_M + f\langle \sigma_{ij} \rangle_\Omega \tag{12}$$

Substituting Eqs. (3), (4) and (7)–(9) into (12), yields

$$\langle \sigma_{ij} \rangle_C = C_{ijmn}(\varepsilon^0_{mn} - f\varepsilon^*_{mn}) \tag{13}$$

Furthermore, several steps of manipulation the Eq. (13) reduces to

$$\langle \sigma_{ij} \rangle = C_{ijmn}\varepsilon^0_{mn} \tag{14}$$

where the effective elastic moduli C_{ijmn} are obtained as

$$C_{ijmn} = C^1_{ijab}\left[I_{abmn} + fV^{-1}_{abqr}\left(C^2_{qrmn} - C^1_{qrmn}\right)\right] \tag{15}$$

The above results are based upon the assumption that the principal axes of the inhomogeneity coincide with the crystalline directions of the matrix (Huang and Kuo, 1996). For a spatially oriented inclusion in a generally anisotropic medium, its orientation can be described by three *Euler angles* θ, ϕ and ω as depicted in Fig. 2. Suppose that $\mathbf{u}_1$, $\mathbf{u}_2$ and $\mathbf{u}_3$ are the unit vectors in the (x, y, z) coordinates and $\bar{\mathbf{u}}_1$, $\bar{\mathbf{u}}_2$ and $\bar{\mathbf{u}}_3$ are the unit vectors in the $(\bar{x}, \bar{y}, \bar{z})$ coordinates, respectively. The overbar denotes quantities associated with the

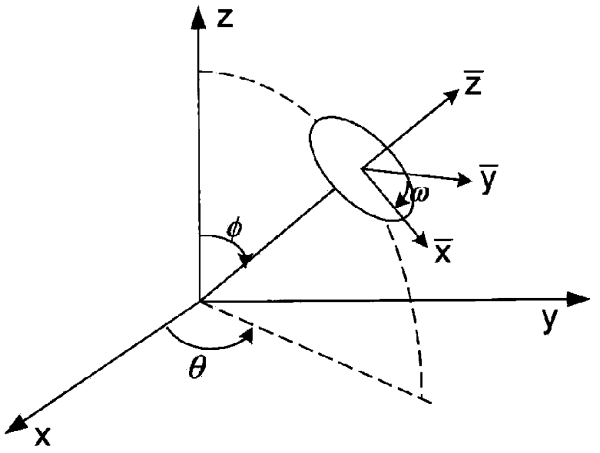

Fig. 2. Representation of Euler angles.

principal directions $(\bar{x}, \bar{y}, \bar{z})$ of the inclusion. The relations between these two sets of unit vectors can be expressed as

$$\begin{Bmatrix} \bar{\mathbf{u}}_1 \\ \bar{\mathbf{u}}_2 \\ \bar{\mathbf{u}}_3 \end{Bmatrix} = [\boldsymbol{\lambda}] \begin{Bmatrix} \mathbf{u}_1 \\ \mathbf{u}_2 \\ \mathbf{u}_3 \end{Bmatrix} \tag{16}$$

where $[\boldsymbol{\lambda}]$ is the direction cosine matrix. According to the above definition of the rotational angles, the matrix is then given by

$$[\boldsymbol{\lambda}] = \begin{bmatrix} mpr - ns & npr + ms & -qr \\ -mps - nr & mr - nps & qs \\ mq & nq & p \end{bmatrix} \tag{17}$$

where $m = \cos(\theta)$, $n = \sin(\theta)$, $p = \cos(\phi)$, $q = \sin(\phi)$, $r = \cos(\omega)$, and $s = \sin(\omega)$.

For a randomly oriented fiber reinforcement composite, the effective moduli depend on the fiber orientation distribution and can be defined by the following integration

$$E_{ijmn} = \int_0^{2\pi}\int_0^{\pi}\int_0^{2\pi} \overline{C}_{ijmn}(\theta, \phi, \omega)\rho(\theta, \phi, \omega) \sin\phi \, \mathrm{d}\omega \, \mathrm{d}\phi \, \mathrm{d}\theta \tag{18}$$

where $\rho(\theta, \phi, \omega)$ is the probability density function of the fibers and $\sin\phi$ is to account for the surface area of a sphere, and $\overline{C}_{ijmn}(\theta, \phi, \omega) = \lambda_{ik}\lambda_{jl}\lambda_{mp}\lambda_{nq}C_{klpq}$.

If the fibers are uniformly distributed over the given region as shown in Fig. 3, then the probability density function $\rho(\theta, \phi, \omega)$ is constant over the region and the corresponding distribution region is defined by

$$-\theta_0 \leqslant \theta \leqslant \theta_0, \quad \frac{\pi}{2} - \phi_0 \leqslant \phi \leqslant \frac{\pi}{2} + \phi_0, \quad 0 \leqslant \omega \leqslant 2\pi \tag{19}$$

where θ_0 and ϕ_0 are prescribed values and ω is given so that any fiber is free to rotate with respect to its direction. Then, the corresponding density function is found to be

$$\rho(\theta, \phi, \omega) = \frac{1}{8\pi\theta_0 \sin\phi_0} \tag{20}$$

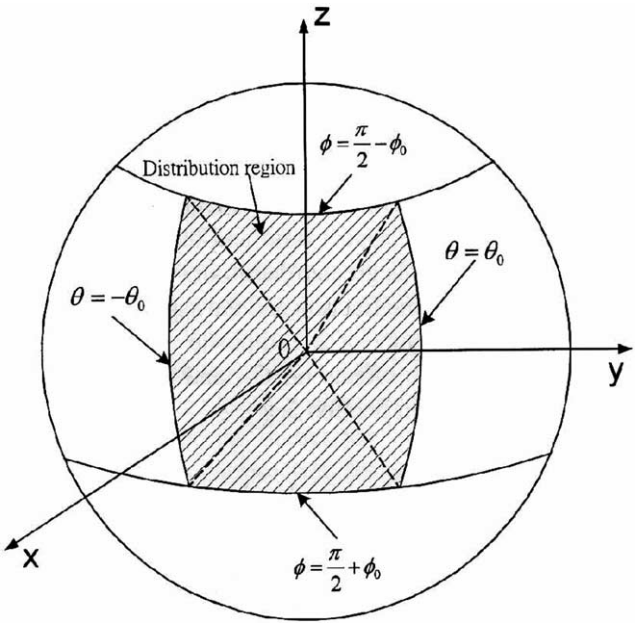

Fig. 3. Fiber distributions in a preferred direction.

Thus, Eq. (18) becomes

$$E_{ijmn} = \frac{1}{8\pi\theta_0 \sin\phi_0} \int_0^{2\pi}\int_0^{\pi}\int_0^{2\pi} \overline{C}_{ijmn}(\theta,\phi,\omega)\sin\phi \,\mathrm{d}\omega\,\mathrm{d}\phi\,\mathrm{d}\theta \tag{21}$$

The explicit result of the integration in Eq. (21) can be obtained for any given θ_0, ϕ_0, and ω_0, since the solution for the effective elastic moduli $\overline{C}_{ijmn}(\theta,\phi,\omega)$ of the composite can be obtained explicitly.

Three special cases of fiber orientations are considered in the present study and they are

Case 1: $\theta_0 \to 0$ and $\phi_0 \to 0$. It represents the special case in which all fibers are aligned and parallel to the x axis and fibers are free to rotate only with respect to three axial directions. The nonzero terms are

$$\begin{aligned} &E_{11} = E_{33}, \quad E_{22} = \frac{\overline{C}_{11} + \overline{C}_{12}}{2}, \quad E_{12} = E_{13} = \overline{C}_{12} \\ &E_{23} = \overline{C}_{12}, \quad E_{44} = \overline{C}_{66}, \quad E_{55} = E_{66} = \overline{C}_{44} \end{aligned} \tag{22}$$

It can be shown that the composite includes only five independent elastic constants. This implies that yz-plane is the plane of isotropy and the composite is macroscopically homogeneous and transversely isotropic.

Case 2: $\theta_0 = \pi$ and $\phi_0 \to 0$. It represents the case in which the fibers are uniformly lying in the xy-plane and it is therefore a two dimensional in-plane distribution. The nonzero terms are

$$\begin{aligned} &E_{11} = E_{22} = E_{33} = \frac{1}{2}\overline{C}_{11} + \frac{1}{2}\overline{C}_{33} - \frac{1}{8}H, \quad E_{12} = \overline{C}_{13} + \frac{1}{8}H \\ &E_{23} = E_{13} = \frac{1}{2}\overline{C}_{13} + \frac{1}{2}\overline{C}_{12}, \quad E_{44} = E_{55} = \frac{\overline{C}_{44} + \overline{C}_{66}}{2} \\ &E_{66} = \frac{1}{2}\overline{C}_{44} + \frac{1}{8}H \end{aligned} \tag{23}$$

where $H = \overline{C}_{11} + \overline{C}_{33} - 2\overline{C}_{23} - 4\overline{C}_{44}$. It can be readily shown that xy-plane is the plane of isotropy and the composite is transversely isotropic with respect to z axis.

Case 3: $\theta_0 = \pi$ and $\phi_0 \to \frac{\pi}{2}$. It represents the case in which fibers are uniformly distributed in all directions, which may be termed as completely random distribution. The composite behavior should be independent of direction or the composite is isotropic. The nonzero terms are

$$\begin{aligned} E_{11} &= E_{22} = E_{33} = \frac{1}{3}(2\overline{C}_{11} + \overline{C}_{33}) - \frac{2}{15}H \\ E_{12} &= E_{23} = E_{13} = \frac{1}{3}(2\overline{C}_{13} + \overline{C}_{12}) + \frac{1}{15}H \\ E_{44} &= E_{55} = E_{66} = \frac{1}{3}(2\overline{C}_{44} + \overline{C}_{66}) + \frac{1}{15}H \end{aligned} \tag{24}$$

Due to symmetric distribution of fiber orientation, the composite as a whole is macroscopically isotropic.

2.2. Equations of motion

Employing the first-order shear deformation theory, the displacement field at a point in the composite laminated plate is expressed as

$$\begin{aligned} U(x,y) &= u_0(x,y) + z\theta_x(x,y) \\ V(x,y) &= v_0(x,y) + z\theta_y(x,y) \\ W(x,y) &= w_0(x,y) \end{aligned} \tag{25}$$

where $u_0(x,y)$, $v_0(x,y)$, $w_0(x,y)$ are the displacement at a point on the mid-plane of the plate, and $\theta_x(x,y)$, $\theta_y(x,y)$ are the rotations of xz and yz planes, respectively. The strain displacement relations due to von-Karman nonlinear kinematics are given as

$$\boldsymbol{\varepsilon} = \boldsymbol{\varepsilon}_0 + z\boldsymbol{\kappa} \tag{26}$$

where

$$\begin{aligned} \boldsymbol{\varepsilon} &= [\,\varepsilon_x \quad \varepsilon_y \quad \gamma_{xy} \quad \gamma_{yz} \quad \gamma_{xz}\,]^{\mathrm{T}} \\ \boldsymbol{\varepsilon}_0 &= \boldsymbol{\varepsilon}_0^{\mathrm{l}} + \boldsymbol{\varepsilon}_0^{\mathrm{nl}} \\ \boldsymbol{\varepsilon}_0^{\mathrm{l}} &= [\,u_{0,x} \quad v_{0,y} \quad u_{0,y} + v_{0,x} \quad w_{0,y} + \psi_y \quad w_{0,x} + \psi_x\,]^{\mathrm{T}} \\ \boldsymbol{\varepsilon}_0^{\mathrm{nl}} &= \left[\,\tfrac{1}{2}(w_{0,x})^2 \quad \tfrac{1}{2}(w_{0,y})^2 \quad w_{0,x}w_{0,y} \quad 0 \quad 0\,\right]^{\mathrm{T}} \\ \boldsymbol{\kappa} &= [\,\psi_{x,x} \quad \psi_{y,y} \quad \psi_{x,y} + \psi_{y,x} \quad 0 \quad 0\,]^{\mathrm{T}} \end{aligned} \tag{27}$$

where superscripts l and nl stands for linear and nonlinear, respectively.

The fiber reinforced composite plate with n layers is assumed to be rectangular with dimensions a, b, and total thickness h. The origin of the coordinates is at the center of the plate. The constitutive equation for an orthotropic lamina with plane stress condition and transverse shear is given by

$$\begin{Bmatrix} \sigma_x \\ \sigma_y \\ \tau_{xy} \\ \tau_{yz} \\ \tau_{xz} \end{Bmatrix} = \begin{bmatrix} E_{11} & E_{12} & E_{16} & 0 & 0 \\ E_{12} & E_{22} & E_{26} & 0 & 0 \\ E_{16} & E_{26} & E_{66} & 0 & 0 \\ 0 & 0 & 0 & E_{44} & E_{45} \\ 0 & 0 & 0 & E_{45} & E_{55} \end{bmatrix} \begin{Bmatrix} \varepsilon_x \\ \varepsilon_y \\ \gamma_{xy} \\ \gamma_{yz} \\ \gamma_{xz} \end{Bmatrix} \tag{28}$$

The force and moment resultants of a composite laminated plate made up of n layers of orthotropic lamina are expressed as

$$\begin{Bmatrix} N_x \\ N_y \\ N_{xy} \\ M_x \\ M_y \\ M_{xy} \end{Bmatrix} = \begin{bmatrix} A_{11} & A_{12} & A_{16} & B_{11} & B_{12} & B_{16} \\ A_{12} & A_{22} & A_{26} & B_{12} & B_{22} & B_{26} \\ A_{16} & A_{26} & A_{66} & B_{16} & B_{26} & B_{66} \\ B_{11} & B_{12} & B_{16} & D_{11} & D_{12} & D_{16} \\ B_{12} & B_{22} & B_{26} & D_{12} & D_{22} & D_{26} \\ B_{16} & B_{26} & B_{66} & D_{16} & D_{26} & D_{66} \end{bmatrix} \begin{Bmatrix} u_{0,x} + \frac{1}{2}(w_{0,x})^2 \\ v_{0,y} + \frac{1}{2}(w_{0,y})^2 \\ u_{0,y} + v_{0,x} + w_{0,x}w_{0,y} \\ \psi_{x,x} \\ \psi_{y,y} \\ \psi_{x,y} + \psi_{y,x} \end{Bmatrix} \tag{29}$$

$$\begin{Bmatrix} Q_y \\ Q_x \end{Bmatrix} = \begin{bmatrix} A_{44} & A_{45} \\ A_{45} & A_{55} \end{bmatrix} \begin{Bmatrix} \gamma_{yz} \\ \gamma_{xz} \end{Bmatrix} \tag{30}$$

The laminate stiffness coefficients (A_{ij}, B_{ij}, D_{ij}) in terms of the reduced stiffness coefficients $(E_{ij})_k$ given in Eq. (21), for the layers $k = 1, 2, \ldots, n$, are defined as

$$(A_{ij}, B_{ij}, D_{ij}) = \sum_{k=1}^{n} \int_{z_{k-1}}^{z_k} (1, z, z^2)(E_{ij})_k \, \mathrm{d}z \quad (i, j = 1, 2, 6) \tag{31}$$

$$A_{ij} = \sum_{k=1}^{n} k_i k_j \int_{z_{k-1}}^{z_k} (E_{ij})_k \, \mathrm{d}z \quad (i, j = 4, 5) \tag{32}$$

where $k_4^2 = \frac{5}{6}$ and $k_5^2 = \frac{5}{6}$ are shear correction factors.

Using the Hamilton's principle, the equations of motion of the plate subjected to transient loading can be derived and are compactly expressed in nondimensional form as

$$(\mathbf{L}_a + \mathbf{L}_b + \mathbf{L}_c)\mathbf{d} + \mathbf{p} = \mathbf{L}_\rho \ddot{\mathbf{d}} \tag{33}$$

where

$$\begin{aligned} \mathbf{L}_a &= \mathbf{L}_{a1}\frac{\partial^2}{\partial x^2} + \mathbf{L}_{a2}\frac{\partial^2}{\partial y^2} + \mathbf{L}_{a3}\frac{\partial^2}{\partial x \partial y} + \mathbf{L}_{a4}\frac{\partial}{\partial x} + \mathbf{L}_{a5}\frac{\partial}{\partial y} + \mathbf{L}_{a6} \\ \mathbf{L}_b &= \mathbf{L}_{b1}\frac{\partial^2}{\partial x^2} + \mathbf{L}_{b2}\frac{\partial^2}{\partial y^2} + \mathbf{L}_{b3}\frac{\partial^2}{\partial x \partial y} \\ \mathbf{L}_c &= \mathbf{L}_{c1}\frac{\partial^2}{\partial x^2} + \mathbf{L}_{c2}\frac{\partial^2}{\partial y^2} + \mathbf{L}_{c3}\frac{\partial^2}{\partial x \partial y} \\ \mathbf{d} &= [\,u \quad v \quad w \quad \psi_x \quad \psi_y\,]^{\mathrm{T}} \\ \mathbf{p} &= [\,0 \quad 0 \quad q \quad 0 \quad 0\,]^{\mathrm{T}} \end{aligned} \tag{34}$$

The 5×5 matrices $\mathbf{L}_{ai}$, $\mathbf{L}_{bi}$, $\mathbf{L}_{ci}$, $\mathbf{L}_d$, and $\mathbf{L}_\rho$ appearing in the preceding equations are given in Appendix A.

2.3. Boundary conditions

The clamped or simply supported boundary conditions at the edges of the plate are expressed as

$$\begin{aligned} \text{Clamped (C):} \quad & \text{At } x = -a/2 \text{ and } a/2, \quad u = v = w = \psi_x = \psi_y = 0 \\ & \text{At } y = -b/2 \text{ and } b/2, \quad u = v = w = \psi_x = \psi_y = 0 \\ \text{Simply supported (S):} \quad & \text{At } x = -a/2 \text{ and } a/2, \quad u = v = w = M_x = \psi_y = 0 \\ & \text{At } y = -b/2 \text{ and } b/2, \quad u = v = w = \psi_x = M_y = 0 \end{aligned}$$

3. Method of solution

A general function $\varphi(x,y)$ is approximated in space domain by finite degree Chebyshev polynomials (Shukla and Nath, 2000) as

$$\varphi(x,y) = \delta \sum_{i=0}^{M} \sum_{j=0}^{M} \varphi_{ij} T_i(x) T_j(y) \tag{35}$$

where

$$\begin{aligned} &\delta = 0.25 \quad \text{if } i = 0 \text{ and } j = 0 \\ &\delta = 0.5 \quad \text{if } i = 0 \text{ and } j \neq 0 \quad \text{or} \quad i \neq 0 \text{ and } j = 0 \\ &\delta = 1 \quad \text{otherwise} \end{aligned}$$

The spatial derivative of a general function $\varphi(x,y)$ can be expressed as

$$\varphi^{rs}_{,xy} = \delta \sum_{i=0}^{M-r} \sum_{j=0}^{N-s} \varphi^{rs}_{ij} T_i(x) T_j(y) \tag{36}$$

where r and s are the order of derivatives with respect to x and y, respectively. Using the recurrence relations (Fox and Parker, 1968), the derivative function φ^{rs}_{ij} is evaluated as

$$\begin{aligned} \varphi^{rs}_{(i-1)j} &= \varphi^{rs}_{(i+1)j} + 2i\varphi^{(r-1)s}_{ij} \\ \varphi^{rs}_{i(j-1)} &= \varphi^{rs}_{i(j+1)} + 2j\varphi^{r(s-1)}_{ij} \end{aligned} \tag{37}$$

The displacement functions and their derivatives can be approximated by finite degree Chebyshev polynomials using Eqs. (35)–(37).

The nonlinear terms appearing in the equations of the motion of the plate due to the product of the dependent variables are linearized at any step of marching variable using quadratic extrapolation technique. A typical nonlinear function $G(x,y)$ at step J is expressed as

$$G_J = \left[\delta \sum_{i=0}^{M-r} \sum_{j=0}^{N} \varphi^{r}_{ij} T_i(x) T_j(y) \right]_J \times \left[\delta \sum_{i=0}^{M} \sum_{j=0}^{N-s} \varphi^{s}_{ij} T_i(x) T_j(y) \right]_J \tag{38}$$

where

$$(\varphi_{ij})_J = \eta_1 (\varphi_{ij})_{J-1} + \eta_2 (\varphi_{ij})_{J-2} + \eta_3 (\varphi_{ij})_{J-3} \tag{39}$$

During initial steps of marching variables, the coefficients η_1, η_2, and η_3 of the quadratic extrapolation scheme of linearization take the following values

$$\begin{aligned} &J = 1 : \eta_1 = 1, \eta_2 = 0, \eta_3 = 0 \\ &J = 2 : \eta_1 = 2, \eta_2 = -1, \eta_3 = 0 \\ &J \geqslant 3 : \eta_1 = 3, \eta_2 = -3, \eta_3 = 1 \end{aligned}$$

Several implicit and explicit schemes of time marching have been used for analyzing dynamic problems. The most common implicit schemes are: Houbolt, Newmark-β, and Wilson-θ. Stricklin et al. (1971) have reported that Houbolt scheme is considered to be best in few studies and Johnson (1966) has shown that it is unconditionally stable for linear problems. However, the Houbolt scheme contaminate the results by artificial damping (Bathe and Wilson, 1976). In the present study, Houbolt implicit time marching scheme

(Houbolt, 1950) is employed to evaluate the inertia terms $\mathbf{L}_\rho\ddot{\mathbf{d}}$ in the governing equations of motion. At time step J, the general acceleration $(\varphi_{,\tau\tau})_J$ is evaluated as

$$(\varphi_{,\tau\tau})_J = (\beta_1\varphi_J + \beta_2\varphi_{J-1} + \beta_3\varphi_{J-2} + \beta_4\varphi_{J-3} + \beta_5)/(\Delta\tau^2) \tag{40}$$

where τ is the nondimensional time period and the Houbolt coefficients β_i's for step loading at different time steps are given as

$$\beta_1 = 6, \beta_2 = 0, \beta_3 = 0, \beta_4 = 0, \beta_5 = -2Q\Delta\tau^2 \quad \text{for } J = 1$$
$$\beta_1 = 2, \beta_2 = -4, \beta_3 = 0, \beta_4 = 0, \beta_5 = -Q\Delta\tau^2 \quad \text{for } J = 2$$
$$\beta_1 = 2, \beta_2 = -5, \beta_3 = 4, \beta_4 = 0, \beta_5 = 0 \quad \text{for } J = 3$$
$$\beta_1 = 2, \beta_2 = -5, \beta_3 = 4, \beta_4 = -1, \beta_5 = 0 \quad \text{for } J \geqslant 3$$

The displacement functions and loading can be approximated by finite degree Chebyshev polynomials as in Eq. (35) and substituting them into Eq. (33) and using the Eqs. (36)–(40), the nonlinear differential equations are linearized and discretized in space and time domain. In the present study total linearization by evaluating the nonlinear terms at each step of marching variable and adding them to the load vector is adopted. Thus the nonlinear differential equation is converted into a system of linear algebraic equations, which are expressed as

$$\sum_{i=0}^{M-2}\sum_{j=0}^{N-2} F_k(u_{ij}, v_{ij}, w_{ij}, \psi_{xij}, \psi_{yij}, P_{ij})T_i(x)T_j(y) = 0 \quad (k = 1, 5) \tag{41}$$

Similarly the appropriate boundary conditions are discretized.

The total number of unknown coefficients is $5(M+1)(N+1)$. Collocating the zeroes of Chebyshev polynomials, $5(M-1)(N-1)$ algebraic equations are generated from Eq. (41). Similarly the CCCC (all edges clamed) and CCSS (two opposite edges clamped and two simply supported) boundary conditions generates $(10M + 10N + 20)$, $(10M + 10N + 18)$ algebraic equations, respectively. Total number of equations become $5(M+1)(N+1) + 20$ and $5(M+1)(N+1) + 18$ for CCCC and CCSS boundary conditions, respectively, which are more than the number of unknown coefficients to be evaluated. The system of linear equations is written in matrix form as

$$\mathbf{Ad} = \mathbf{p} \tag{42}$$

To ensure the uniqueness of the solution of Eq. (42) multiple regression analysis based on least square error norm is carried out. Finally, the system of linear equations is expressed in matrix form as

$$\mathbf{d} = (\mathbf{A}^{\mathrm{T}}\mathbf{A})^{-1}\mathbf{A}^{\mathrm{T}}\mathbf{p} \tag{43}$$

The coefficients of the displacement vectors are evaluated at each step and from which using Eq. (35) the displacement at any point in the plate is computed.

4. Results and discussion

In the present study, the nonlinear governing equations of motion of composite laminated rectangular plates containing spatially oriented short fibers and subjected to time dependent uniform transverse loading are solved using the fast converging double Chebyshev polynomials and Houbolt time marching scheme. In order to have a check on the accuracy and stability of the present methodology of the solution, spatial and temporal convergence studies are carried and are shown in Figs. 4 and 5, respectively. It is found that nine terms expansion of the variables in Chebyshev series and an increment of 0.1 for nondimensional time τ are

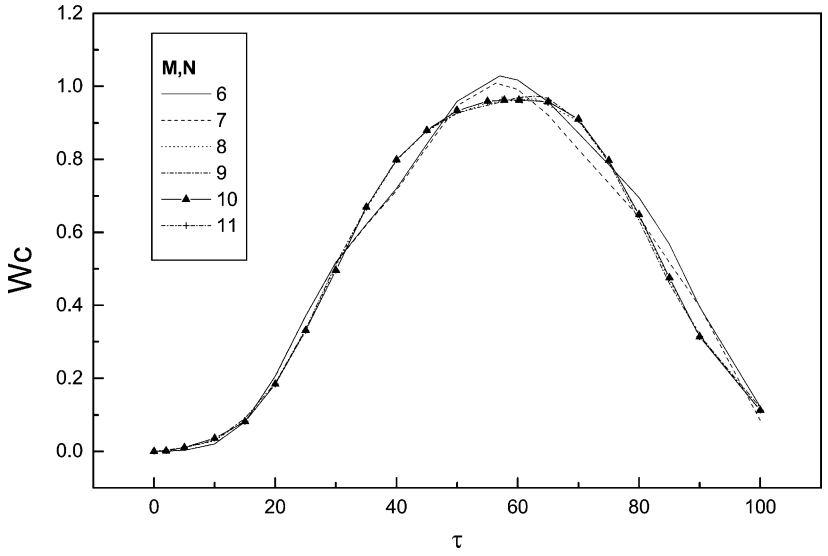

Fig. 4. Spatial convergence of the transverse central displacement of [0/90/0/90] CCCC plate ($a_3/a_1 = 4$, $f = 0.1$, $\beta = 120$, Case 1, $\Delta\tau = 0.1$).

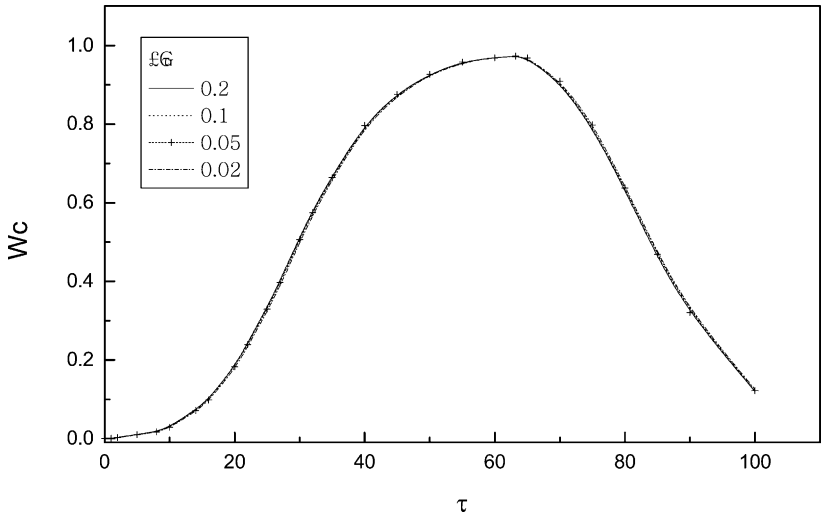

Fig. 5. Temporal convergence of the transverse central displacement of [0/90/0/90] CCCC plate ($a_3/a_1 = 4$, $f = 0.1$, $\beta = 120$, Case 1).

sufficient to yield satisfactory results. An iterative approach with relative convergence criteria of 0.01% of each coefficient at every iteration across each step is employed. The present methodology is also validated by comparing the plate center displacement (W_c) and moment of a thin isotropic simply supported plate under uniform transverse dynamic loading presented by Akay (1980) using the finite element method and shown in Table 1. It is observed that the results are in good comparison.

The numerical results for E-glass/Epoxy fiber reinforced laminates are presented. The elastic properties used for the calculations are $C_{11}^1 = 8.23$ GPa, $C_{12}^1 = 4.24$ GPa, $v^1 = 0.34$ for epoxy matrix, and $C_{11}^2 = 83.34$ GPa, $C_{12}^2 = 23.51$ GPa, $v^2 = 0.22$ for E-glass fibers. It is assumed that all layers of the laminated plate have

Table 1
Comparison of central deflection and moment of thin isotropic plate ($a = 243.8$ cm, $h = 0.635$ cm, $v = 0.25$; $E = 7.031 \times 10^5$ kg/cm^2, $\rho = 2.547 \times 10^{-6}$ kg s^2/cm^4, $q(x, y, t) = 4.882 \times 10^{-4}$ kg/cm^2)

Load level	Center			
	W_c (Max) (cm)		M_x (Max) (kg cm/cm)	
	Present	Akay (1980)	Present	Akay (1980)
q	0.5781	0.6014	1.9248	1.9704
$5q$	1.2139	1.2607	3.7885	3.6149
$10q$	1.6694	1.6337	5.7436	5.4295

the same thickness and fiber volume fraction. The nondimensional uniform step load $Q = 50$ is taken in the study for all the cases. The nonlinear dynamic responses of composite cross-ply and angle-ply laminated plates with spatially oriented short fibers are presented for different fiber volume fraction, fiber aspect ratio, and fiber orientation in the composites.

Figs. 6–9 show the effect of fiber orientation on the central displacement (W_c) response of four layers antisymmetric cross-ply [0/90/0/90], symmetric cross-ply [0/90/90/0], antisymmetric angle-ply [45/−45/45/−45], and unsymmetric [0/15/30/45] laminated plates with fiber volume fraction $f = 0.1$ and fiber aspect ratio $a_3/a_1 = 4$, respectively. It is observed that maximum peak transverse central deflection is lowest for fiber orientation Case 3, when the fibers are completely randomly distributed for all the four laminated composite plates. For fiber orientation Cases 1 and 2, it is almost same. The effect of uniform distribution of the fibers in the composites on the nonlinear dynamic response is more than other fiber distributions.

The effect of fiber aspect ratio (a_3/a_1) on the nonlinear displacement response of a four layers antisymmetric cross-ply laminated CCCC square plate with fiber volume fraction $f = 0.1$, fiber orientation Case 1 and plate span to thickness ratio $\beta\ (= a/h) = 40$ is shown in Fig. 10. It is observed that with increase in the fiber aspect ratio the resistance of the composite plate against transient loading increases and the amplitude of the motion of the plate is least for composite containing long fibers ($a_3/a_1 = 32$) and highest for composite containing short fibers ($a_3/a_1 = 2$). However, the displacement responses corresponding to

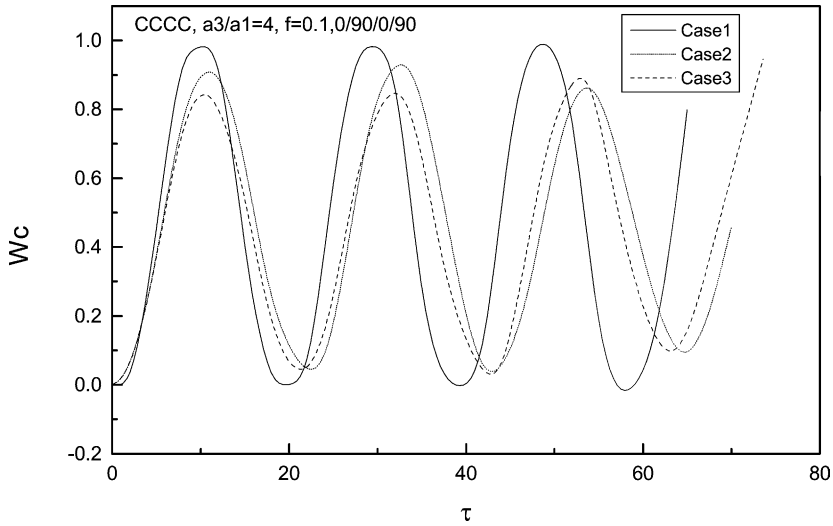

Fig. 6. Effect of fiber orientation on the dynamic response of four layers antisymmetric cross-ply CCCC plate ($a_3/a_1 = 4$, $f = 0.1$, $\beta = 20$).

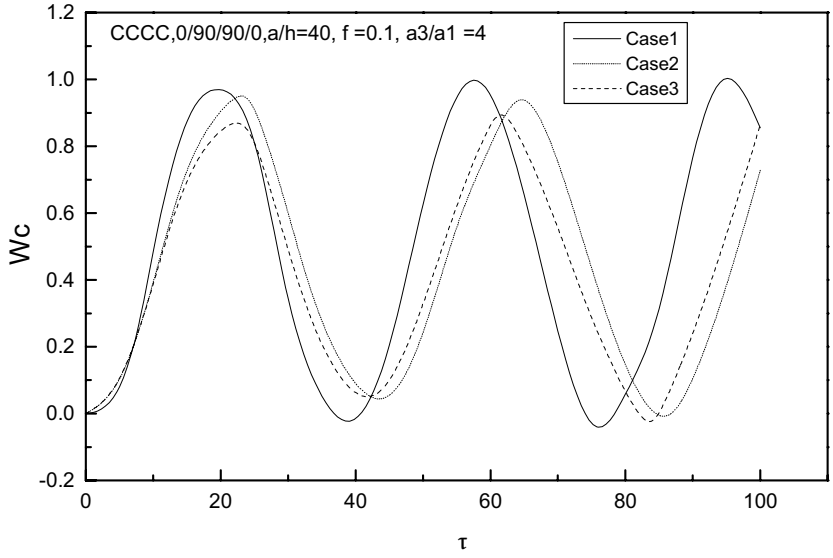

Fig. 7. Effect of fiber orientation on the dynamic response of four layers symmetric cross-ply CCCC plate ($a_3/a_1 = 4$, $f = 0.1$, $\beta = 40$).

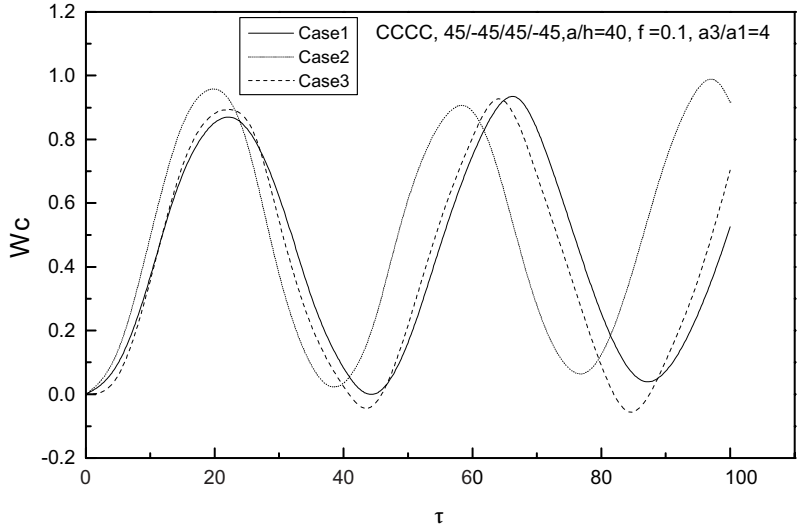

Fig. 8. Effect of fiber orientation on the dynamic response of four layers antisymmetric angle-ply [45/−45/45/−45] CCCC plate ($a_3/a_1 = 4$, $f = 0.1$, $\beta = 40$).

fiber aspect ratio 16 and 32 are almost same indicating that at this value of the fiber aspect ratio, the fibers in the composites behave as long fibers.

Fig. 11 depicts the effect of fiber volume fraction in the fiber orientation Case 1 containing short fibers ($a_3/a_1 = 4$) on the dynamic response of the laminated composite [0/90/0/90] CCCC plate ($a/h = 40$). It is

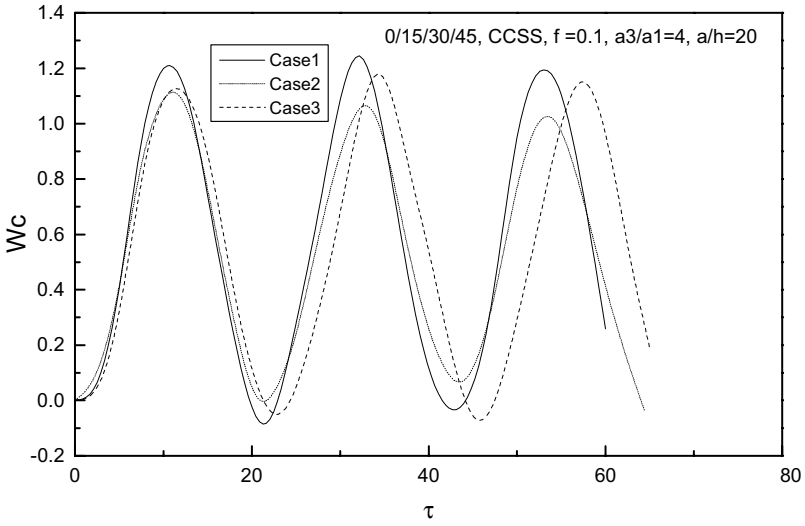

Fig. 9. Effect of fiber orientation on the dynamic response of four layers unsymmetrically laminated [0/15/30/45] CCSS plate ($a_3/a_1 = 4$, $f = 0.1$, $\beta = 20$).

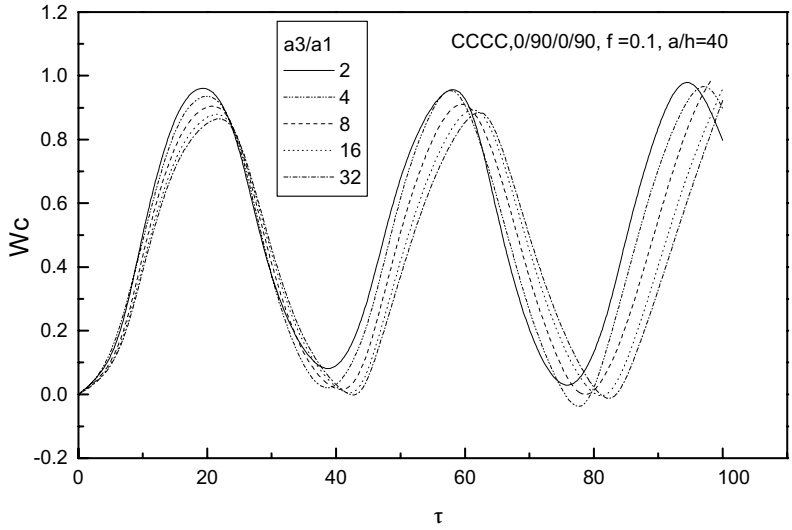

Fig. 10. Effect of fiber aspect ratio on the dynamic response of four layers antisymmetric cross-ply CCCC plate ($f = 0.1$, $\beta = 40$, Case 1).

observed as expected that with increase in the fiber volume fraction the amplitude of the plate motion decreases but the frequency of the motion remains almost same.

Fig. 12 reveals that the effect of lamination scheme in case of composite laminated plate containing short fibers with fiber volume fraction $f = 0.1$ and fiber orientation Case 1 on the nonlinear displacement response of the CCSS square plate ($a/h = 20$). It is observed that maximum peak displacement and frequency of the motion is almost same for cross-ply and angle-ply symmetric, antisymmetric and unsymmetric

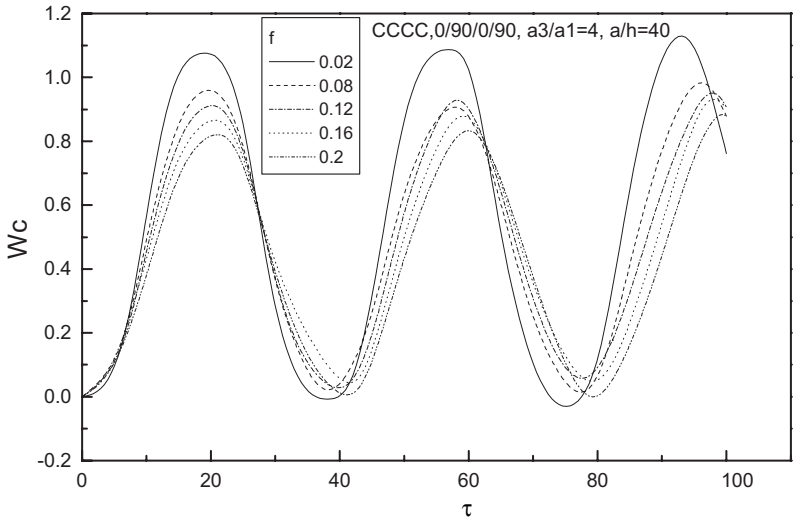

Fig. 11. Effect of fiber volume fraction on the dynamic response of four layers antisymmetric cross-ply CCCC plate ($a_3/a_1 = 4$, $\beta = 40$, Case 1).

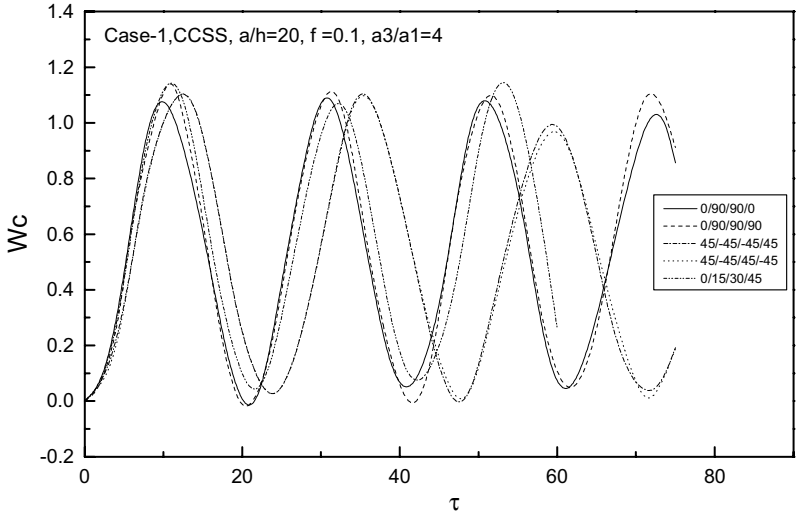

Fig. 12. Effect of lamination scheme on the dynamic response of CCSS plate ($a_3/a_1 = 4$, $f = 0.1$, $\beta = 20$, Case 1).

laminated plates. The lamination scheme does not affect the displacement response in case of composite with short fibers aligned such that the composite is macroscopically homogeneous and transversely isotropic.

Fig. 13 shows the effect of plate span to thickness ratio on the transient displacement response of the [0/90/0/90] CCCC plate with short fibers aligned and parallel to the x axis which are free to rotate only with respect to three axial directions. As in the case of composites with long fibers, the frequency of the motion increases with decrease in the plate span to thickness ratio. However, the amplitude remains almost same.

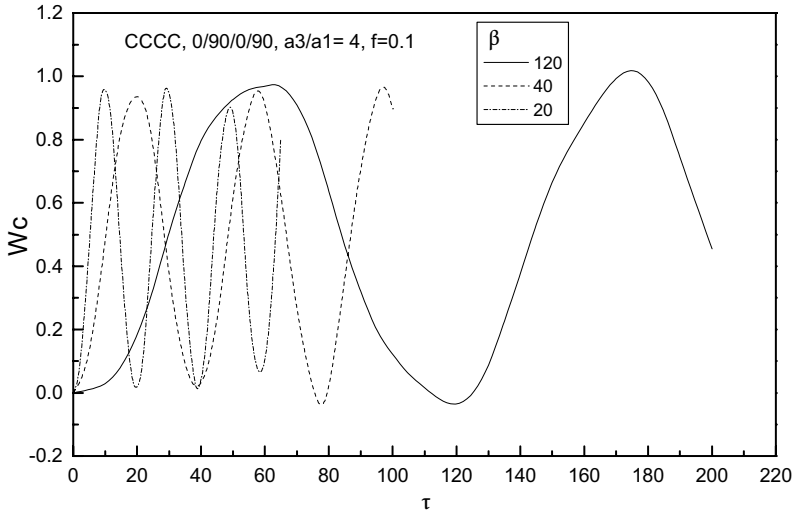

Fig. 13. Effect of plate thickness ratio a/h on the dynamic response of four layers antisymmetric cross-ply CCCC plate ($a_3/a_1 = 4$, $f = 0.1$, Case 1).

5. Conclusions

The nonlinear dynamic responses for laminated composite plates composed of spatial short fibers subjected to uniform transverse transient loading are obtained. It is observed that with increase in the short fiber volume fraction, the amplitude decreases but the frequency does not change. It is also found that amplitude of the motion is higher for short fibers and it decreases when the fibers in the composite are long. The fibers orientation in the composites with spatial short fibers influence the response of the plate and it is found that the maximum peak displacement of the plate is lower when the fibers are uniformly distributed in the composites, i.e., completely random distribution of short fibers. However, no significant difference in the displacement response is observed in case of symmetric, antisymmetric, unsymmetric cross-ply, and angle-ply laminated plate with short fibers.

Acknowledgements

The authors gratefully acknowledge the financial support by the National Science Council of Taiwan, Republic of China (Contract Nos. NSC 90-2212-E-035-004, 90-2745-P-035-004, 91-2212-E-035-008, and 91-2811-E035-001).

Appendix A

The nondimensional parameters appearing in the governing equations are defined as

$$\lambda = \frac{a}{b}, \quad \beta = \frac{a}{h}, \quad x = \frac{2X}{a}, \quad y = \frac{2Y}{b}$$

$$u = \frac{u_0}{h}, \quad v = \frac{v_0}{h}, \quad w = \frac{w_0}{h}, \quad \overline{N}_x = \frac{N_x \beta}{A_{11}}$$

$$\overline{N}_y = \frac{N_y\beta}{A_{22}}, \quad \overline{N}_{xy} = \frac{N_{xy}\beta}{A_{66}}, \quad \overline{M}_x = \frac{M_x h\beta^2}{D_{11}}, \quad \overline{M}_y = \frac{M_y h\beta^2}{D_{22}}$$
$$\overline{M}_{xy} = \frac{M_{xy} h\beta^2}{D_{66}}, \quad Q = \frac{qa^4}{C_{11}^1 h^4}, \quad \tau = t\sqrt{\frac{4A_{22}}{Pa^2}} \tag{A.1}$$

The matrices defined in Eq. (34) are expressed as follows

$$\mathbf{L}_{a1} = \begin{bmatrix} 1 & \frac{A_{16}}{A_{11}} & 0 & \frac{B_{11}}{hA_{11}} & \frac{B_{16}}{hA_{11}} \\ \frac{A_{16}}{A_{22}} & \frac{A_{66}}{A_{22}} & 0 & \frac{B_{16}}{hA_{22}} & \frac{B_{66}}{hA_{22}} \\ 0 & 0 & \frac{A_{55}}{A_{22}} & 0 & 0 \\ \frac{hB_{11}}{D_{11}} & \frac{hB_{16}}{D_{11}} & 0 & 1 & \frac{D_{16}}{D_{11}} \\ \frac{hB_{16}}{D_{22}} & \frac{hB_{66}}{D_{22}} & 0 & \frac{D_{16}}{D_{22}} & \frac{D_{66}}{D_{22}} \end{bmatrix}$$

$$\mathbf{L}_{a2} = \begin{bmatrix} \frac{\lambda^2 A_{66}}{A_{11}} & \frac{\lambda^2 A_{26}}{A_{11}} & 0 & \frac{\lambda^2 B_{66}}{hA_{11}} & \frac{\lambda^2 B_{26}}{hA_{11}} \\ \frac{\lambda^2 A_{26}}{A_{22}} & \lambda^2 & 0 & \frac{\lambda^2 B_{26}}{hA_{22}} & \frac{\lambda^2 B_{22}}{hA_{22}} \\ 0 & 0 & \frac{\lambda^2 A_{44}}{A_{22}} & 0 & 0 \\ \frac{h\lambda^2 B_{66}}{D_{11}} & \frac{h\lambda^2 B_{26}}{D_{11}} & 0 & \frac{\lambda^2 D_{66}}{D_{11}} & \frac{\lambda^2 D_{26}}{D_{11}} \\ \frac{h\lambda^2 B_{26}}{D_{22}} & \frac{h\lambda^2 B_{22}}{D_{22}} & 0 & \frac{\lambda^2 D_{26}}{D_{22}} & \lambda^2 \end{bmatrix}$$

$$\mathbf{L}_{a3} = \begin{bmatrix} \frac{2\lambda A_{16}}{A_{11}} & \frac{\lambda(A_{12}+A_{66})}{A_{11}} & 0 & \frac{2\lambda B_{16}}{hA_{11}} & \frac{\lambda(B_{12}+B_{66})}{hA_{11}} \\ \frac{\lambda(A_{12}+A_{66})}{A_{22}} & \frac{2\lambda A_{26}}{A_{22}} & 0 & \frac{\lambda(B_{12}+B_{66})}{hA_{22}} & \frac{2\lambda B_{26}}{hA_{22}} \\ 0 & 0 & \frac{2\lambda A_{45}}{A_{22}} & 0 & 0 \\ \frac{2h\lambda B_{16}}{D_{11}} & \frac{h\lambda(B_{12}+B_{66})}{D_{11}} & 0 & \frac{2\lambda D_{16}}{D_{11}} & \frac{\lambda(D_{12}+D_{66})}{D_{11}} \\ \frac{h\lambda(B_{12}+B_{66})}{D_{22}} & \frac{2h\lambda B_{26}}{D_{22}} & 0 & \frac{\lambda(D_{12}+D_{66})}{D_{22}} & \frac{2\lambda D_{26}}{D_{22}} \end{bmatrix}$$

$$\mathbf{L}_{a4} = \begin{bmatrix} 0 & 0 & 0 & 0 & 0 \\ 0 & 0 & 0 & 0 & 0 \\ 0 & 0 & 0 & \frac{\beta A_{55}}{2A_{22}} & \frac{\beta A_{45}}{2A_{22}} \\ 0 & 0 & -\frac{h^2\beta A_{55}}{2D_{11}} & 0 & 0 \\ 0 & 0 & -\frac{h^2\beta A_{45}}{2D_{22}} & 0 & 0 \end{bmatrix}$$

$$\mathbf{L}_{a5} = \begin{bmatrix} 0 & 0 & 0 & 0 & 0 \\ 0 & 0 & 0 & 0 & 0 \\ 0 & 0 & 0 & \frac{\lambda\beta A_{45}}{2A_{22}} & \frac{\lambda\beta A_{44}}{2A_{22}} \\ 0 & 0 & -\frac{h^2\lambda\beta A_{45}}{2D_{11}} & 0 & 0 \\ 0 & 0 & -\frac{h^2\lambda\beta A_{44}}{2D_{22}} & 0 & 0 \end{bmatrix}$$

$$\mathbf{L}_{a6} = \begin{bmatrix} 0 & 0 & 0 & 0 & 0 \\ 0 & 0 & 0 & 0 & 0 \\ 0 & 0 & 0 & 0 & 0 \\ 0 & 0 & 0 & -\frac{h^2\beta^2 A_{55}}{4D_{11}} & -\frac{h^2\beta^2 A_{45}}{4D_{11}} \\ 0 & 0 & 0 & -\frac{h^2\beta^2 A_{45}}{4D_{22}} & -\frac{h^2\beta^2 A_{44}}{4D_{22}} \end{bmatrix}$$

$$\mathbf{L}_{\rho} = \begin{bmatrix} \frac{A_{22}}{A_{11}} & 0 & 0 & \frac{A_{22}R}{A_{11}Ph} & 0 \\ 0 & 1 & 0 & 0 & \frac{R}{Ph} \\ 0 & 0 & 1 & 0 & 0 \\ \frac{A_{22}Rh}{D_{11}P} & 0 & 0 & \frac{A_{22}I}{D_{11}P} & 0 \\ 0 & \frac{A_{22}Rh}{D_{22}P} & 0 & 0 & \frac{A_{22}I}{D_{22}P} \end{bmatrix} \tag{A.2}$$

where P, R, and I are the normal, coupled normal rotary, and rotary inertia coefficients, respectively. They are defined as

$$(P, R, I) = \int_{-h/2}^{h/2} \rho(1, z, z^2)\mathrm{d}z \tag{A.3}$$

The entries of the matrices $\mathbf{L}_{b1}$, $\mathbf{L}_{b2}$, $\mathbf{L}_{b3}$, $\mathbf{L}_{c1}$, $\mathbf{L}_{c2}$, and $\mathbf{L}_{c3}$ are zero except

$$\mathbf{L}_{b2}(1,3) = \frac{2\lambda^2}{\beta A_{11}}(A_{66}w_{,x} + \lambda A_{26}w_{,y})$$

$$\mathbf{L}_{b2}(2,3) = \frac{2\lambda^2}{\beta A_{22}}(A_{26}w_{,x} + \lambda A_{22}w_{,y})$$

$$\mathbf{L}_{b2}(3,3) = \frac{2\lambda^2}{\beta A_{22}}(A_{12}u_{,x} + \lambda A_{26}u_{,y} + A_{26}v_{,x} + \lambda A_{22}v_{,y}) + \frac{2\lambda^2}{h\beta A_{22}}(B_{12}\psi_{x,x} + \lambda B_{26}\psi_{x,y} + B_{26}\psi_{y,x} + \lambda B_{22}\psi_{y,y})$$

$$\mathbf{L}_{b2}(4,3) = \frac{2h\lambda^2}{\beta D_{11}}(B_{66}w_{,x} + \lambda B_{26}w_{,y})$$

$$\mathbf{L}_{b2}(5,3) = \frac{2h\lambda^2}{\beta D_{22}}(B_{26}w_{,x} + \lambda B_{22}w_{,y})$$

$$\mathbf{L}_{b3}(1,3) = \frac{2\lambda}{\beta A_{11}}\{2A_{16}w_{,x} + \lambda(A_{12} + A_{66})w_{,y}\}$$

$$\mathbf{L}_{b3}(2,3) = \frac{2\lambda}{\beta A_{22}}\{(A_{12} + A_{66})w_{,x} + 2\lambda A_{26}w_{,y}\}$$

$$\mathbf{L}_{b3}(3,3) = \frac{4\lambda}{\beta A_{22}}\{A_{16}u_{,x} + \lambda A_{66}u_{,y} + A_{66}v_{,x} + \lambda A_{26}v_{,y}\} + \frac{1}{h}(B_{16}\psi_{x,x} + \lambda B_{66}\psi_{x,y} + B_{66}\psi_{y,x} + \lambda B_{26}\psi_{y,y})$$

$$\mathbf{L}_{b3}(4,3) = \frac{2h\lambda}{\beta D_{11}}\{2B_{16}w_{,x} + \lambda(B_{12} + B_{66})w_{,y}\}$$

$$\mathbf{L}_{b3}(5,3) = \frac{2h\lambda}{\beta D_{22}}\{(B_{12} + B_{66})w_{,x} + 2\lambda B_{26}w_{,y}\}$$

$$\mathbf{L}_{c1}(3,3) = \frac{2}{\beta^2 A_{22}}\{A_{11}(w_{,x})^2 + \lambda^2 A_{12}(w_{,y})^2 + 2\lambda A_{16} w_{,x} w_{,y}\}$$

$$\mathbf{L}_{c2}(3,3) = \frac{2\lambda^2}{\beta^2 A_{22}}\{A_{12}(w_{,x})^2 + \lambda^2 A_{22}(w_{,y})^2 + 2\lambda A_{26} w_{,x} w_{,y}\} \tag{A.4}$$

$$\mathbf{L}_{c3}(3,3) = \frac{4\lambda}{\beta^2 A_{22}}\{A_{16}(w_{,x})^2 + \lambda^2 A_{26}(w_{,y})^2 + 2\lambda A_{66} w_{,x} w_{,y}\}$$

References

Akay, H.U., 1980. Dynamic large deflection analysis of plates using mixed finite elements. Computers and Structures 11, 1–11.

Bathe, K.J., Wilson, E.L., 1976. Numerical Methods in Finite Element Analysis. Prentice Hall Inc, New Jersey.

Beveniste, Y., 1987. A new approach to the application of Mori–Tanaka's theory to the composite materials. Mechanics of Material 6, 147–157.

Bhimaraddi, A., 1992. Nonlinear free vibration of laminated composite plates. ASCE Journal of Engineering Mechanics 118 (1), 1874–1891.

Cheng, Z.Q., Wang, X.X, Huang, M.G., 1993. Nonlinear flexural vibration of rectangular moderately thick plates and sandwich plates. International Journal of Mechanical Sciences 35, 815–827.

Christensen, R.M., Malls, W.F., 1972. Effective stiffness of randomly oriented fiber composites. Journal of Composite Materials 6, 518–532.

Eshelby, J.D., 1957. The determination of the elastic field of an ellipsoidal inclusion and related problems. Proceedings of the Royal Society of London A 241, 376–396.

Fox, L., Parker, I.B., 1968. Chebyshev Polynomials in Numerical Analysis. Oxford University Press, London.

Halpin, J.C., Jerine, K., Whitney, J.M., 1971. The laminate analogy for two and three dimensional composite materials. Journal of Composite Materials 5, 36–49.

Houbolt, J.C., 1950. A recurrence matrix solution for the dynamic response of the elastic aircraft. Journal of Aeronautical Sciences 17, 540–550.

Huang, J.H., 2001. Dynamic analysis of laminated plates containing randomly oriented reinforcements. Composites: Part A 32, 1573–1582.

Huang, J.H., Kuo, W.S., 1996. Micromechanics determination of the effective properties of piezoelectric composites containing spatially oriented short fibers. Acta Metallurgica 44 (2), 4889–4898.

Johnson, D.E., 1966. A proof of the stability of the Houbolt method. AIAA J. 4, 1450–1451.

Khdeir, A.A., Reddy, J.N., 1999. Free vibration of laminated composite plates using second-order shear deformation theory. Computers and Structures 71, 617–626.

Leissa, A.W., 1998. The plates and shell vibration monographs. Applied Mechanics Review 51 (10), R19–R28.

Mori, T., Tanaka, K., 1973. Average stress in matrix and average energy of materials with misfitting inclusions. Acta Metallurgica 21, 571–574.

Mura, T., 1987. Micromechanics of Defects in Solids, second ed. Martinus Nijhoff, Dordrecht.

Nath, Y., Shukla, K.K., 2001. Nonlinear transient analysis of moderately thick laminated composite plates. Journal of Sound and Vibration 247, 509–526.

Reddy, J.N., 1983. Dynamic (transient) analysis of layered anisotropic composite material plates. International Journal of Numerical Mechanical Engineering 19, 237–255.

Rivilin, T., 1974. The Chebyshev Polynomials. John Wiley & Sons, New York.

Sathyamoorthy, M., 1987. Nonlinear vibration analysis of plates: a review and survey of current developments. Applied Mechanics Review 40, 1553–1561.

Shi, Y., Lee, R.Y.Y., Mei, C., 1997. Finite element method for nonlinear free vibration of composite plates. American Institute of Aeronautics and Astronautics Journal 35, 159–166.

Shukla, K.K., Nath, Y., 2000. Nonlinear analysis of moderately thick laminated rectangular plates. Journal of Engineering Mechanics, ASCE 126 (8), 831–838.

Singh, G., Rao, G.V., 2000. A lock free material finite element for nonlinear oscillations of laminated plates. Journal of Sound and Vibration 230, 221–240.

Stricklin, J.A., Martinez, J.E., Tillerson, J.R., Hong, J.H., Haisler, W.E., 1971. Nonlinear dynamic analysis of shells of revolution by matrix displacement method. AIAA J. 9, 629–636.

Taya, M., Chou, T.W., 1981. On two kinds of ellipsoidal inhomogeneities in an infinite elastic body. International Journal of Solids and Structures 17, 553–563.

Weng, G.J., 1990. The theoretical connection between Mori–Tanaka's theory and the Hashin–Shtrikman–Walpole bounds. International Journal of Engineering Science 28 (11), 1111–1120.

Yamada, G., Irie, T., 1987. Plate vibration research in Japan. Applied Mechanics Review 40, 879–892.